FASTENER PULL-THROUGH FAILURE IN GFRP LAMINATES

G. Catalanotti[1*], P.P. Camanho[1], P. Ghys[2], A.T. Marques[1]
[1] DEMec, Faculdade de Engenharia, Universidade do Porto, Rua Dr. Roberto Frias, 4200-465, Porto, Portugal
[2] ALSTOM Transport, 48 Rue Albert Dhalenne, 93482, Saint-Ouen, France
* Corresponding author(giuseppe.catalanotti@fe.up.pt)

Keywords: *Hybrid structures, Bolted joints*

1 Intoduction

GFRP laminates are used in marine, railway and automotive industries in non-structural parts and, more recently, in main load-carrying structures.

The use of composites leads to a reduction of the weight (and consequently of the cost of the transportation), a reduction of the manufacturing cost (simplification of the design and reduction of the cost required for the assembly), and to a reduction of the recurring cost (composites require less maintenance than metals).

Due to their high specific stiffness and strength and to the flexibility in their use, GFRP are nowadays used together with metals in the design of hybrid low-cost train structures. Hybrid structures are interesting for the industry because they can bring a gain in mass of about 12-24% and a gain in cost of about 20 [1]. One of the main design requirements of the railway industry is the calculation of the strength of hybrid bolted joints which correspond to the critical region of the structures.

While the prediction of the strength of composite bolted joints under in-plane failure mechanism has been thoroughly investigated in the literature [2–5], few attempts have been made to predict out-of-plane failure mechanism such as fastener pull through [6–9] and practically inexistent those regarding the GFRP laminates.

The aim of this paper is to study experimentally the fastener pull-through failure mode in GFRP laminates and to propose a numerical technique to predict the response of a bolted joint. Taking into account that in industrial applications several resins are used to satisfy the current legislation (and in particular about the burning behavior [11]) the study presented here concerns two different resins: the phenolic and the vinylester.

2 Experiments

2.1 Materials

The composites investigated in this study are: Fiber Glass-vinylester composite (GF-V); Fiber Glass-phenolic composite (GF-P). The laminates were manufactured using the technique of resin infusion and they have the quasi-isotropic lay-up reported in Table 1.

Table 1: Orientation pattern for GF-vinylester / phenolic composite.

ply	type of product	supplier
14	±45 − 610 g/m2	SELCOM
13	90 − 600 g/m2	GAZECHIM
12	±45 − 610 g/m2	SELCOM
11	90 − 600 g/m2	GAZECHIM
10	±45 − 610 g/m2	SELCOM
9	0 − 1246 g/m2	SELCOM
8	±45 − 610 g/m2	SELCOM
7	±45 − 610 g/m2	SELCOM
6	0 − 1246 g/m2	SELCOM
5	±45 − 610 g/m2	SELCOM
4	90 − 600 g/m2	GAZECHIM
3	±45 − 610 g/m2	SELCOM
2	90 − 600 g/m2	GAZECHIM
1	±45 − 610 g/m2	SELCOM
	isoftalic poliester gelcoat	POLYPROCESS

The mechanical properties of these laminates are reported in Table 2 where E_1 is the longitudinal Young's modulus, E_2 is the transverse Young's modulus, v_{12} is the Poisson's ratio in direction 12, v_{13} is the Poisson's ratio in direction 13 and G_{12} is the shear modulus.

The material was tested after a heat aging treatment according to the AFNOR norm [12].

Table 2: Mechanical properties of UD laminates.

materials	GF-vinylester	GF-phenolic
E_1 (MPa)	42830	35200
E_2 (MPa)	1530	3000
v_{12}	0.35	0.35
v_{13}	0.3	0.3
G_{12} (MPa)	2800	3400
G_{13} (MPa)	2800	3400

2.2 Description of the test

The pull-through test is performed following the norm ASTMD7332 Standard Test Method for Measuring the Fastener Pull-Through Resistance of a Fiber-Reinforced Polymer Matrix Composite [10]. This test method proposes two procedures, A and B. Since procedure A is more complex and has inherent problems associated with the flexural stiffness of the specimen to test, the specimens procedure B is used. The test was conducted using an INSTRON-4208 test machine. Figure 1 shows the experimental set-up used.

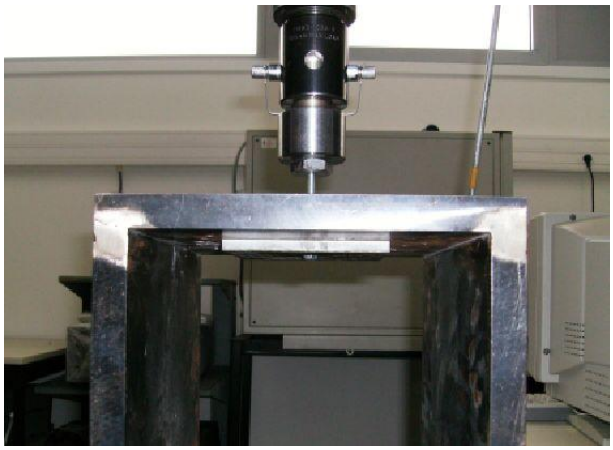

Fig.1. Equipment set-up for PT test.

The testing machine was equipped with a 100kN load cell. The speed of the machine (displacement controlled test) was 2mm/min. The temperature of the room was 23ºC and the relative humidity was 50% for all the duration of the tests.
After each test the damaged specimen was examined and the type of failure was identified.

The test results depend on Clearance Hole parameter (C_b). This is the diameter of the plate that it is used in procedure B of the test. In the tests performed C_b was taken as 30mm. For each specimen are reported the dimensions, the ratio of the Clearance Hole Diameter C_b to Fastener Hole Diameter d, and the ratio of the Fastener Hole Diameter to the thickness of the specimen (h). The test specimens are square plates with a length of 105mm.

2.3 Derived properties

The load-displacement for a pull-through test is used to identify three important characteristics of the joint that are:

- the Initial Sub-Critical Failure Load: the load at the first sub-critical failure of the specimen;
- the Initial Sub-Critical Failure Displacement: the displacement at the first sub-critical failure of the specimen;
- the Failure Load: the maximum load attained in the test.

The specimen shows a first failure mode (generally delamination) at a relatively low load. After delamination, the specimen is able to support increasing loads. This point is identified in the curve by a changing of the linearity and by a load-drop.

2.4 GF-phenolic specimens

Table 3 reports the dimensions of the specimens and the geometric parameters of the equipment used.

Table 3 : GF-P specimens' dimensions.

Specimen	Diameter (mm)	C_b/D	h (mm)	D/h
PT-P-6	6	5	6.8	0.882
PT-P-10	10	3	6.8	1.471

Table 4: Pull-trough test, results for PT-P-6 specimens.

Specimen	In. Sub-crit. load (N)	Failure load (N)	In. Sub-crit. displ. (mm)
PT-P-6-1(*)	12340	17348	1.228
PT-P-6-2(*)	11752	17236	1.301
PT-P-6-3(*)	12384	17132	1.36
Mean	12158	17238	1.296
STDV	352	108	0.066

(*) bolt failure

Three specimens were tested for eqch configuration: one with 6mm and the other with 10mm diameter hole. Figure 2 shows the plots of the load vs. displacement curves for the phenolic specimens. Figure 2(a) shows the curves for PT-P-6 while Figure 2(b) show the curves for PT-P-10. In Table 4-5 the derived properties for the specimen tested are reported.
It should be noted that some specimens exhibited bolt failure.

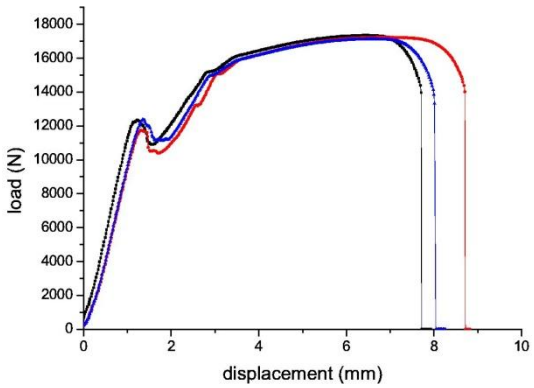

(a) PT-P-6

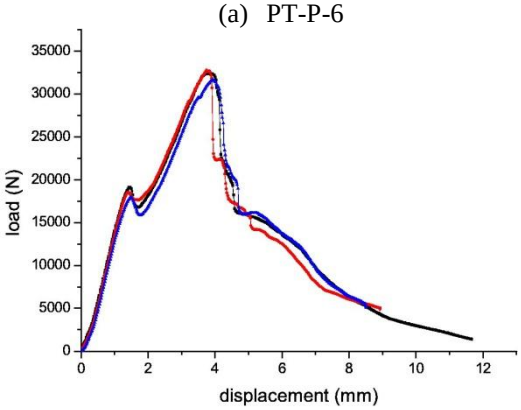

(b) PT-P-10

Fig. 2. Load vs. displacement for GF-phenolic specimens.

Table 5: Pull-trough test, results for PT-P-10 specimens.

Specimen	In. Sub-crit. load (N)	Failure load (N)	In. Sub-crit. displ. (mm)
PT-P-10-1	19140	32460	1.462
PT-P-10-2	18528	32780	1.403
PT-P-10-3	17976	31608	1.492
Mean	18548	32282	1.452
STDV	582	605	0.045

2.5 GF-vinylester specimens

Table 6 reports the dimensions of the specimens and the geometric parameters of the equipment used.
Three specimens were tested for eqch configuration: one with 6mm and the other with 10mm diameter hole.
Figure 3 shows the plots of the load vs. displacement curves for the vinylester specimens.

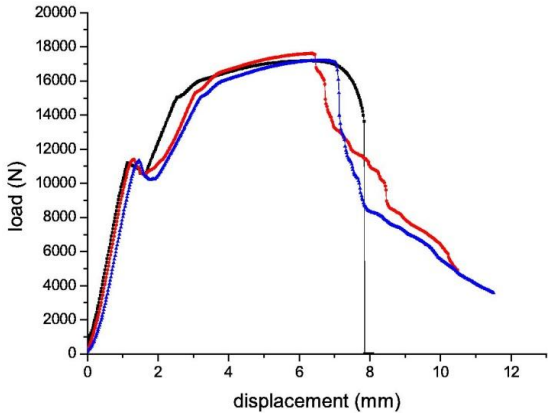

(a) PT-V-6

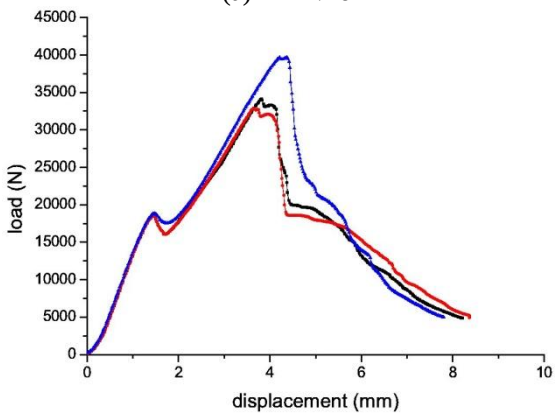

(b) PT-V-10

Fig. 3. Load vs. displacement for GF- vinylester specimens.

Table 6: GF-V specimens' dimensions.

Specimen	Diameter (mm)	C_b/D	h (mm)	D/h
PT-V-6	6	5	6.8	0.882
PT-V-10	10	3	6.8	1.493

Figure 3(a) shows the curves for PT-V-6 while Figure 3(b) shows the curves for PT-V-10. In Table 7-8 the derived properties for the specimen tested are reported.

Table 7: Pull-trough test, results for PT-V-6 specimens.

Specimen	In. Sub-crit. load (N)	Failure load (N)	In. Sub-crit. displ. (mm)
PT-V-6-1(*)	11200	17184	1.127
PT-V-6-2	11404	17624	1.315
PT-V-6-3	11340	17204	1.463
Mean	11314	17337	1.302
STDV	104	248	0.168

(*) bolt failure

Table 8: Pull-trough test, results for PT-V-10 specimens.

Specimen	In. Sub-crit. load (N)	Failure load (N)	In. Sub-crit. displ. (mm)
PT-V-10-1	18448	34172	1.447
PT-V-10-2	18920	32864	1.44
PT-V-10-3	18876	39692	1.477
Mean	18748	35576	1.455
STDV	260	3624	0.02

2.6 Damaged-zones

Figure 4, shows the delamination that occurs at the sub-critical failure load near the hole. If the load increases, the intralaminar fracture in the material starts and, at the end, the specimen is totally penetrated by the washer. The delamination occurs abruptly when the sub-critical initial load is reached.

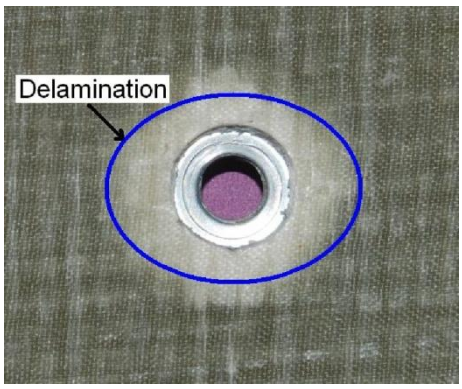

Fig. 4. Pull-trough specimens after loading.

As this phenomenon interest several plies, it is not possible to identify with certain knowledge where occurs the first delamination crack even is it seems probable that they occurs at the interface with the thick 0º plies.

2.7 Comparison of the PT test results

Figure 5 shows the failure loads of the materials tested. As expected, increasing the diameter increases both the sub-initial critical failure load and the failure load of the specimen. The results show that the material exhibit slight differences in the values of the two failure loads considered. It should be also noted that increasing the diameter also increases the ratio between the initial sub-critical failure load to the ultimate failure load.

This means that larger holes exhibit an initial sub-critical failure load that is relatively lower when compared to the ultimate failure load.

Moreover, it is noticed that after the sub-critical initial failure load the compliance of the specimen is constant and that means that the intra-laminar damage is negligible when the load is lower than the failure load. This behavior is in contrast with that observed in CFRP laminates [7,9]. For this reason, the FE model proposed in the following for the prediction of the sub-critical initial failure load neglects the intralaminar damage of the material and do consider only the eventual delamination.

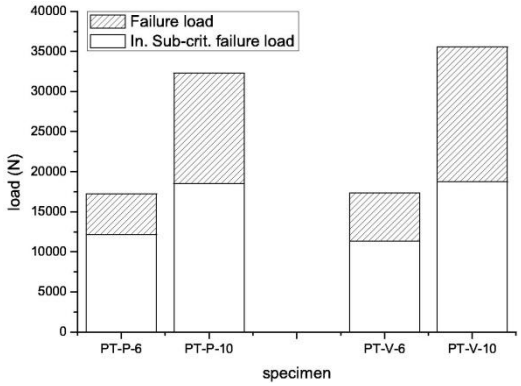

Fig. 5. Comparison of PT tests failure loads.

3 Numerical model

It was concluded in the previous section that the design load should be the sub-critical failure load because after this value the joint can be considered damaged. To predict this load in the numerical model will be used cohesive elements together with linear elastic elements. As the results are similar for the different materials, this means that the interface strengths and the fracture toughnesses are the same and therefore only the pull-through test of the phenolic specimens will be studied numerically.

3.1 Comparison of the PT test results

The Finite Element model, done using Abaqus6.8 [13], is shown in Figure 6. The specimen and the bolt (screw and washers) are modeled as deformable bodies while the steel plate used for the pull-through test is modeled as an analytical surface. Frictionless contact is considered between the different parts.

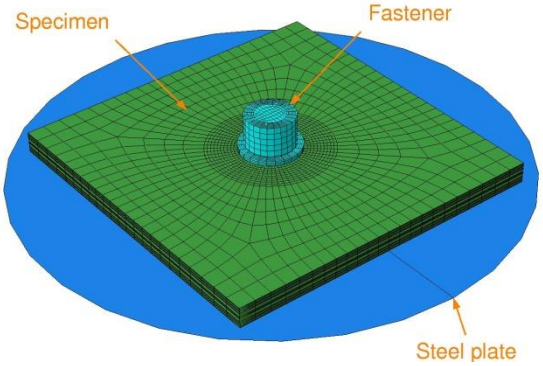

Fig. 6. FE model of the pull-through test (top view).

The specimen was modeled using 8-nodes linear brick reduced integration elements (CRD8R). The cohesive elements were modeled using collapsed 8-nodes user elements in the between the plies [15]. To reduce the complexity of the model (and the time needed for the analysis) the cohesive elements were used only in the vicinity of the bolt. The relevant parameters for the definition of the cohesive elements were found using experimental data previously obtained for a similar material [14]. For the sake of completeness the results of the interlaminar tests are reported in Table 9.

Table 9: Critical values of SERR (N/mm) [14].

Mode mixture φ	test	G_{IC}^{φ}	G_{IIC}^{φ}	G_C
0	DCB	1.25	0	1.25
0.25	MMB	1.14	0.38	1.52
0.5	MMB	0.97	0.97	1.94
0.75	MMB	0.6	1.81	2.41
1	ENF	0	3.6	3.6

Using these values the semi-empirical exponent [17] reads h = 1.98 and the interface strengths assume the values τ_0^3 = 28.8MPa and τ_{sh}^3 = 48.8MPa.
The interface strengths are calculated using the engineeristic solution proposed in [16]. The element dimension was about 1mm and four elements were considered along the crack.

3.2 Numerical results

Numerical simulations were performed on the GF-P specimen.
Figure 7 shows the contour plot of the transversal stress σ_{33} after the onset of the delamination. It is possible to notice that once that the delamination occurs there is a redistribution of the stress inside the material.

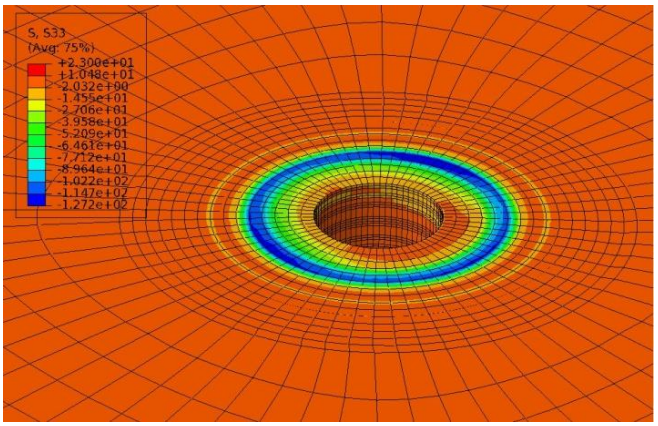

Fig. 7: σ_{33} after the onset of the delamination.

Figure 8 shows the load as a function of the displacement obtained from the numerical analysis.

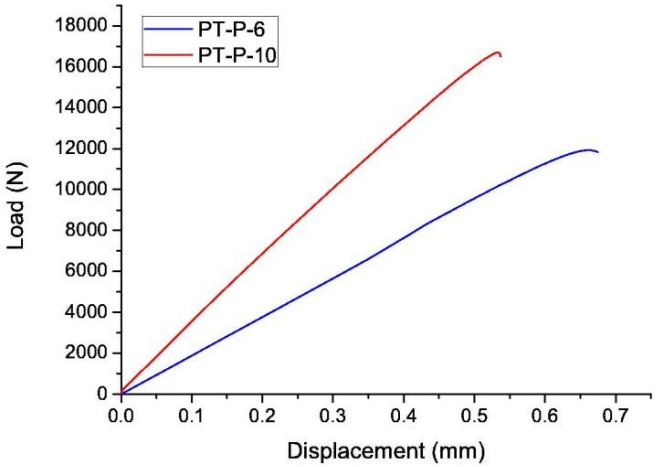

Fig. 8. Predicted load vs. displacement curve.

The predictions for the initial sub-critical failure load and the experimental values are reported in Table 10. A good agreement between numerical prediction and experimental data is found.

Table 10: Sub-critical load: experiments and predictions.

Specimens	Experiments (N)	Numerical (N)	Error (%)
PT-P-6	12158	11922	<2%
PT-P-10	18548	16700	<10%

4 Concluding remarks

In this paper is presented an experimental and a numerical study of the pull-through damage in GFRP laminates. Two different material system (GF-phenolic and GF-vinylester) and two geometries (diameter of the hole 6mm and 10mm) were investigated. It can be concluded that:

- increasing the diameter of the bolt increases both the sub-critical initial failure load and the failure load;
- larger holes exhibit a sub-critical initial failure load that is relatively lower when compared to the ultimate failure load;
- the interlaminar damage is the predominant phenomenon at least when the load is lower than the failure load;
- using three-dimensional finite element models using linear elastic elements together with cohesive elements allows to predict with a reasonable error the value of the sub-critical initial failure load.

References

[1] "Comparaison entre caisses à technologie différent". Alstom Transport. 2008. (in French).

[2] Camanho, P.P. and Matthews, F.L., "Stress analysis and strength prediction in FRP: a review", *Composites - Part A*. 1997; 28:529-547.

[3] Hart-Smith, L.J., "Mechanically-Fastened Joints for Advanced Composites - Phenomenological Considerations and Simple Analysis", *Douglas Paper*. McDonnell Douglas Corporation 1978; 6748:1-32.

[4] Hart-Smith, L.J., 2Design and Analysis of Bolted and Riveted Joints in Fibrous Composite Structures2, *Douglas Paper*. McDonnell Douglas Corporation 1986; 1986:1-15.

[5] Camanho, P.P., Lambert, M., "A design methodology for mechanically fastened joints in laminated composite materials", *Composites Science and Tecnology*. 2006; 66:3004-3020.

[6] Elder, D.J., Verdaasdonk, A.H., Thomson, R.S., "Fastener pull-through in a carbon fibre epoxy composite joint", *Composite Structures*. 2008; 86:291-298.

[7] Banbury, A., Kelly, D.W., "A study of fastener pull-through failure of composite laminates. Part 1: Experimental", *Composite Structures*. 1999; 45:241-254.

[8] Banbury, A., Kelly, D.W., Jain, L.K., "A study of fastener pull-through failure of composite laminates. Part 2: Failure prediction", *Composite Structures*. 1999; 45:255-270.

[9] Kelly, G., Hallström, S., "Strength and failure mechanisms of composite laminates subject to localised transverse loading", *Composite Structures*. 2005; 69:301-314.

[10] ASTM D7332 / D7332M - 09, "Standard Test Method for Measuring the Fastener Pull-Through Resistance of a Fiber-Reinforced Polymer Matrix Composite".

[11] French Norm NF F 16-101:1988. "All vehicles - the burning behavior – materials to choose". 1998, October (original in French).

[12] French Norm NF T 57-107:1986. "Glass-fibre-reinforced plastics – Measurement of the change of characteristics during hot water treatment". 1986, December (original in French).

[13] Abaqus 6.8 Documentation, Dessault Systèmes. 2008.

[14] Tumino, D., Catalanotti, G., Cappello, F., Zuccarello, B., "Experimental tests on fatigue induced delamination in GFRP and CFRP laminates", *Proceedings of ICEM13*, Alexandropulis, Greece, July1-6, 2007.

[15] Turon, A., Camanho, P.P., Costa, J., Dávila, C.G., "A damage model for the simulation of delamination in advanced composites under variable-mode loading", *Mechanics of Materials*. 2006; 38:1072-1089.

[16] Turon, A., Camanho, P.P., Costa, J., Renart, J., "Accurate simulation of delamination growth under mixed-mode loading using cohesive elements: Definition of interlaminar strengths and elastic stiffness", *Composite Structures*. 2010; 92:1857-1864.

[17] Benzeggagh, M.L., Kenane, M., "Measurement of mixed-mode delamination fracture toughness of unidirectional glass/epoxy composites with mixed-mode bending apparatus", *Composite Science and technology*. 1996; 56:439-449.